

On three topical aspects of the $N=28$ isotonic chain

J. Piekarewicz¹

¹*Department of Physics, Florida State University, Tallahassee, FL 32306*

(Dated: November 17, 2018)

Abstract

The evolution of single-particle orbits along the $N = 28$ isotonic chain is studied within the framework of a relativistic mean-field approximation. We focus on three topical aspects of the $N=28$ chain: (a) the emergence of a new magic number at $Z=14$; (b) the possible erosion of the $N=28$ shell; and (c) the weakening of the spin-orbit splitting among low- j neutron orbits. The present model supports the emergence of a robust $Z=14$ subshell gap in ^{48}Ca , that persists as one reaches the neutron-rich isotone ^{42}Si . Yet the proton removal from ^{48}Ca results in a significant erosion of the $N=28$ shell in ^{42}Si . Finally, the removal of $s^{1/2}$ protons from ^{48}Ca causes a $\sim 50\%$ reduction of the spin-orbit splitting among neutron p -orbitals in ^{42}Si .

PACS numbers: 21.10.-k,21.10.Pc,21.60.Jz

I. INTRODUCTION

The study of exotic nuclei is defining a new frontier in nuclear science. The existent nuclear shell model—the powerful theoretical edifice built upon insights developed for over half a century from the study of stable nuclei—may crumble as one leaves the valley of stability and reaches the extremes of nuclear existence. Fundamental nuclear-structure concepts, such as the spin-orbit force and the concomitant emergence of magic numbers, may need to be revised and redefined [1, 2].

Although the atomic nucleus is shaped by the complex interplay between strong, electromagnetic, and weak interactions, the nearly 300 stable nuclei—by their mere existence—probe a relatively small window of the nuclear chart. Yet the advent of Radioactive Ion Beam Facilities (RIBFs) have started to change the nuclear landscape and have offered the first glimpses of exotic new phenomena. One of the central questions that the new generation of RIBFs will attempt to answer is what happens to nuclei at the extreme conditions of isospin where the balance between strong, electromagnetic, and weak interactions differs significantly from that in stable nuclei. And some answers have started to emerge. For example, two exotic nuclei— ^{42}Si [3] and ^{78}Ni [4]—have recently been produced at the National Superconducting Cyclotron of Michigan State University. The most neutron-rich of the doubly-magic nuclei known to date, ^{78}Ni has a proton-to-neutron ratio of $Z/N = 0.56$, considerably smaller than the $Z/N = 0.65$ value for the heaviest of doubly-magic nuclei ^{208}Pb . Further, with twice as many neutrons as protons—and just one neutron away from the drip line— ^{42}Si reaches a proton-to-neutron fraction of only $Z/N = 0.5$. For comparison, the heaviest stable member of the isotopic chain (^{30}Si) has a proton-to-neutron ratio of $Z/N = 0.88$.

Understanding nuclei at the extreme conditions of isospin will also shed light on a variety of fundamental questions in astrophysics, such as the nucleosynthesis of heavy elements and the structure and dynamics of neutron stars. These phenomena depend critically on knowledge of the equation of state of neutron-rich matter which at present is woefully inadequate. For example, in the rapid-neutron capture process (r-process), stable nuclei (such as iron) are exposed to a neutron-rich environment that favors neutron-capture timescales that are considerably shorter than the beta-decay lifetime of the exotic nuclei that are being produced [5]. Both the capture and decay rates depend critically on the shell structure of nuclei far from stability and in particular on the appearance and disappearance of magic numbers [6, 7]. Further, neutron-rich nuclei are expected to develop a neutron skin (or even a neutron halo). Knowledge of the neutron skin of neutron-rich nuclei places important constraints on the equation of state of pure neutron matter [8]. Indeed, the slope of the equation of state of neutron matter—a quantity related to its pressure—has been shown to be strongly correlated to the neutron skin of heavy nuclei [8, 9] which, in turn, is correlated to the structure [10, 11, 12], and cooling [13] of neutron stars.

Motivated by these topical issues, we have organized the manuscript around three questions that pertain to the evolution of single-particle orbits along the $N = 28$ isotonic chain: (a) do relativistic mean-field models support the emergence of a new magic number at proton number $Z = 14$? (b) Does the emergence a new magic number at proton number $Z = 14$ leads to the erosion of the $N = 28$ neutron shell? (c) Is there a significant weakening of the spin-orbit splitting among low- j neutron orbits as one moves from ^{48}Ca to ^{42}Si ?

The first question is motivated by a recent experiment that suggests that the neutron-rich nucleus ^{42}Si is doubly magic and has a (nearly) spherical shape [3]. Yet this result is not

without controversy, as the short β -decay lifetime of ^{42}Si has been suggested by some as evidence in favor of a strong deformation [14].

Theoretically, this issue is equally controversial and strongly coupled to our second question: is there evidence for the possible erosion of the $N = 28$ neutron shell at $Z = 14$? On the one hand, the emergence of a robust subshell closure at $Z = 14$ has been credited with preventing deformation, thereby lending support to the notion that ^{42}Si is indeed a new doubly-magic nucleus [15, 16]. On the other hand, it has been argued that the progressive removal of $1d^{3/2}$ and $2s^{1/2}$ protons causes an erosion of the $N = 28$ neutron shell, resulting in a strong deformation in ^{42}Si [17, 18, 19, 20, 21].

The third question explores the possibility of a significant and systematic weakening of the spin-orbit splitting among the $2p$ -neutron orbitals with proton removal. The first indication of the existence of such an effect in the case of ^{46}Ar was presented in Ref. [22] where it was shown that in a relativistic mean-field approach the spin-orbit splitting depends sensitively on the magnitude of the proton density in the nuclear interior, and in particular on the occupation of $2s_{1/2}$ orbit. Moreover, it was illustrated that ^{46}Ar departs from the long-standing paradigm of a spin-orbit potential proportional to the derivative of the central potential. Since then, this effect has been confirmed experimentally by Gaudefroy, Sorlin, and collaborators by using the $^{46}\text{Ar}(d,p)^{47}\text{Ar}$ transfer reaction in inverse kinematics [23].

A particularly interesting theoretical alternative to the relativistic mean-field approach presented here has been proposed by Otsuka and collaborators [24, 25]. In their approach, the novel evolution of single particle orbits is attributed to the spin-isospin structure of the underlying nucleon-nucleon (NN) interaction—particularly the spin-spin [24] and tensor [25] components. The relativistic mean-field formulation presented here, based solely on scalar and timelike-vector Lorentz structures, does not generate any tensor structure.¹ Yet, it has been shown recently by Serra, Otsuka, and collaborators [26], that a significant contribution from the underlying NN tensor force manifests itself, through renormalization effects, in the scalar-isoscalar component of the relativistic mean field potential (the so-called “ σ -meson” contribution). That such “complicated” effects emerge in such a simple approach may not come as a surprise. The strength of an effective field theory framework is that by fitting a small number of empirical constants to ground-state data, a variety of correlation effects that go beyond the mean-field theory get encoded into the parameters of the model [27]. What requires further insights, however, is the precise role in which the various spin-isospin structures of the bare NN interaction find their way into the empirical constants of the effective field theory.

To address the three questions outlined above, the manuscript has been organized as follows. In Sec. II the effective NL3 Lagrangian is introduced [28, 29] alongside some minor modifications required to describe the physics of the $N = 28$ isotonic chain. This effective Lagrangian is used to compute a variety of ground-state observables at the mean-field level. Further details on the implementation of these techniques may be found in Refs. [30, 31, 32]. In Sec. III, results for the evolution of both neutron and proton single-particle orbits along the $N = 28$ isotonic chain are presented and discussed. We conclude in Sec. IV with a brief summary of our results.

¹ Although the spacelike component of a vector interaction generates a tensor structure, the spacelike component vanishes if a spherical ground state is assumed.

Model	m_s	g_s^2	g_v^2	g_ρ^2	κ	λ
NL3	508.194	104.387	165.585	79.600	3.860	-0.016
NL3	450.000	82.890	165.585	79.600	3.860	-0.016

TABLE I: The original NL3 parameter set (first row) and the modified one (second row) used in the calculations. The modifications are necessary to (approximately) describe the $1d^{3/2}$ - $2s^{1/2}$ proton gap in ^{40}Ca . The parameter κ and the inverse scalar range m_s are given in MeV. The nucleon, omega, and rho masses are kept fixed at $M = 939$ MeV, $m_\omega = 782.5$ MeV, and $m_\rho = 763$ MeV, respectively.

II. FORMALISM

The starting point for the calculation of various ground-state properties is an interacting Lagrangian density of the following form:

$$\mathcal{L}_{\text{int}} = \bar{\psi} \left[g_s \phi - \left(g_v V_\mu + \frac{g_\rho}{2} \boldsymbol{\tau} \cdot \mathbf{b}_\mu + \frac{e}{2} (1 + \tau_3) A_\mu \right) \gamma^\mu \right] \psi - \frac{\kappa}{3!} (g_s \phi)^3 - \frac{\lambda}{4!} (g_s \phi)^4.$$

The Lagrangian density includes an isodoublet nucleon field (ψ) interacting via the exchange of two isoscalar mesons, a scalar (ϕ) and a vector (V^μ), one isovector meson (b^μ), and the photon (A^μ) [30, 31]. In addition to meson-nucleon interactions the Lagrangian density is supplemented by two nonlinear meson interactions with coupling constants denoted by κ and λ . These two terms are instrumental in the softening of the equation of state of symmetric nuclear matter.

A. Ground-state Properties

The NL3 parameter set has been enormously successful at describing a large body of ground-state observables throughout the periodic table [28, 29]. Yet in the present contribution a fine tuning of the NL3 parameters is needed to account for the $1d^{3/2}$ - $2s^{1/2}$ proton gap in ^{40}Ca . Indeed, the original NL3 parameter set predicts a proton gap of 0.83 MeV, while the experimental value has been quoted at 2.8 ± 0.6 [33]. To bring the gap closer to the experimental value an adjustment of the scalar mass m_s is done while maintaining the ratio $C_s^2 \equiv g_s^2 / (m_s/M)^2 / m_s^2$ fixed at $C_s^2 \approx 360$ (see Table I). This prescription ensures that the binding energy and charge radius of ^{40}Ca remain fixed at (or close to) their experimental values (see Table II). As the main goal of the fine tuning is simply to obtain a reasonable $1d^{3/2}$ - $2s^{1/2}$ proton gap in ^{40}Ca , no attempt was made at re-fitting other parameters of the model.

III. RESULTS

Having adjusted the NL3 parameter set to reproduce (approximately) the $1d^{3/2}$ - $2s^{1/2}$ proton gap in ^{40}Ca , we are now in a position to study the evolution of both proton and neutron single-particle spectra along the $N = 28$ isotonic chain.

Nucleus	B/A (MeV)	r_{ch} (fm)	$\epsilon(1d^{5/2})$ (MeV)	$\epsilon(2s^{1/2})$ (MeV)	$\epsilon(1d^{3/2})$ (MeV)
^{40}Ca	8.55	3.52	-15.23 (6.04)	-11.02 (1.83)	-9.19 (0.00)
^{48}Ca	8.71	3.51	-22.91 (5.99)	-17.03 (0.11)	-16.92 (0.00)
^{42}Si	7.41	3.27	-24.41 (6.00)	-19.55 (1.14)	-18.41 (0.00)

TABLE II: Evolution of the the proton single-particle spectrum in the $s-d$ shell. Also shown are binding energies per nucleon and charge radii. Quantities in parenthesis are single-proton energies relative to the $\epsilon(1d^{3/2})$.

A. Proton Spectrum

The evolution of the proton single-particle spectrum as one goes from $^{40}\text{Ca}_{20}$ to $^{42}\text{Si}_{12}$ via $^{48}\text{Ca}_{28}$ is depicted in Fig. 1. The same information (limited to the $s-d$ shell) alongside binding energies per nucleon and root-mean-square charge radii is listed in Table II. The figure is particularly suggestive of a new shell closure at proton number $Z=14$ that emerges from the near-degeneracy between the $2s^{1/2}$ and the $1d^{3/2}$ proton orbitals at neutron number $N=28$ [34]. This critical feature is well accounted for by the relativistic mean-field model. Indeed, the energy gap between the $1d^{3/2}$ and $2s^{1/2}$ proton orbitals is reduced from ~ 2 MeV in ^{40}Ca to a mere 110 keV in ^{48}Ca . This results in a robust 6 MeV energy gap between the $1d^{5/2}$ orbital and the quasi-degenerate pair. This quasi-degeneracy gets only slightly diluted by stripping ^{48}Ca from its six valence protons. In this form, one reaches the “doubly-magic” nucleus ^{42}Si , with a predicted proton gap at the Fermi surface of almost 5 MeV. (Note that the original NL3 parameter set, although accurately calibrated, predicts a $1d^{3/2}$ - $2s^{1/2}$ proton gap in ^{48}Ca of -1.8 MeV.)

The quasi-degeneracy of the $2s^{1/2}$ and the $1d^{3/2}$ orbitals, the main physics behind the appearance of a new magic number at $Z=14$, is related to the old phenomenon of “pseudospin” symmetry. This is a symmetry that manifests itself among $(n+1)lj=l+1/2$ and $n(l+2)j=l+3/2$ orbitals, with $(n-1)$ the number of nodes, l the orbital angular momentum, and j the total angular momentum of the single-particle orbital. Nothing a-priori suggests a symmetry among pseudospin-orbit partners (*e.g.*, $2s^{1/2}$ and $1d^{3/2}$ orbitals), as their wave functions differ in both angular momentum and number of nodes, a feature that is clearly illustrated on the left-hand panel of Fig. 2. Yet pseudo-spin symmetry appears to repair these differences at large separations ($r \gtrsim 5$ fm), leading to an exponential behavior controlled by energies that differ by only 110 keV. We note that while the quantitative value of the $1d^{3/2}$ - $2s^{1/2}$ energy splitting is model dependent, their near-degeneracy is a robust result that is well described within the relativistic approach.

In a series of seminal papers, Ginocchio and collaborators have shown that pseudospin symmetry appears naturally in a relativistic approach as a consequence of the similarity among the “small” (or lower) components of the Dirac orbitals, rather than from a similarity among the dominant upper components. In the particular case of the $2s^{1/2}$ and $1d^{3/2}$ pseudo-spin orbit partners, the lower components carry quantum numbers given by $p^{1/2}$ and $p^{3/2}$, respectively. Thus, both orbitals experience the same centrifugal barrier. Further, because of their respective boundary conditions, they also display the same number of nodes [35]. The only difference among these orbitals arises from the presence of a “small” *pseudospin-orbit* potential that results from the cancellation of large scalar and vector potentials. Note that large scalar and vector potentials are the hallmark of all successful relativistic mean-field theories and the main reason behind the large *spin-orbit* potential, where the large potentials

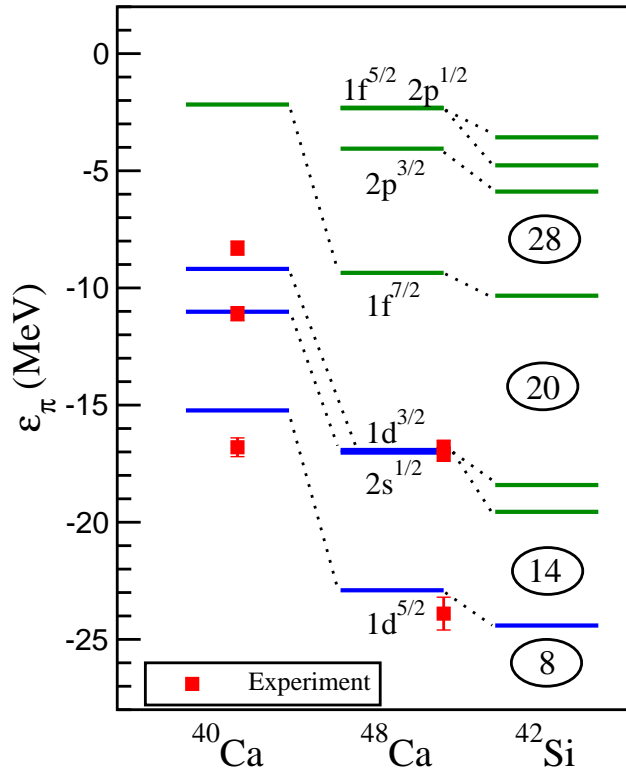


FIG. 1: (color online) Proton single-particle spectrum in ^{40}Ca , ^{48}Ca , and ^{42}Si . Particularly relevant are: (i) the near degeneracy of the $1d^{3/2}$ - $2s^{1/2}$ in ^{48}Ca and (ii) the emergence of a $Z = 14$ gap in ^{48}Ca that seems to persist in ^{42}Si .

add rather than cancel. The uncanny resemblance among the lower components of the $2s^{1/2}$ and $1d^{3/2}$ Dirac spinors is depicted on the right-hand panel of Fig. 2. The role of pseudospin symmetry in exotic nuclei is an interesting topic that deserves further consideration.

B. Neutron Spectrum

In the previous section the evolution of the proton spectrum with increasing neutron number was explored. It was suggested that the filling of the $1f^{7/2}$ neutron orbital in the Calcium isotopes resulted in the appearance of a new magic number at $Z = 14$ that appears to persist as one removes the six valence protons from ^{48}Ca , thereby reaching the “doubly-magic” nucleus $^{42}_{14}\text{Si}_{28}$ [3, 15, 16].

In this section we are interested in exploring a complementary effect, namely, the evolution of the neutron single-particle spectrum in the $N = 28$ isotones as a function of the progressive removal of the six valence protons in ^{48}Ca . Thus, we start this section by displaying in Fig. 3 the neutron counterpart to the proton single-particle spectrum depicted in Fig. 1. Particularly interesting is the prediction that as new magic number emerges at proton number $Z = 14$, an old one disappears at neutron number $N = 28$. While this result is at variance with the conclusions of Refs. [15, 16], it supports the findings of Refs. [17, 18, 19, 20, 21].

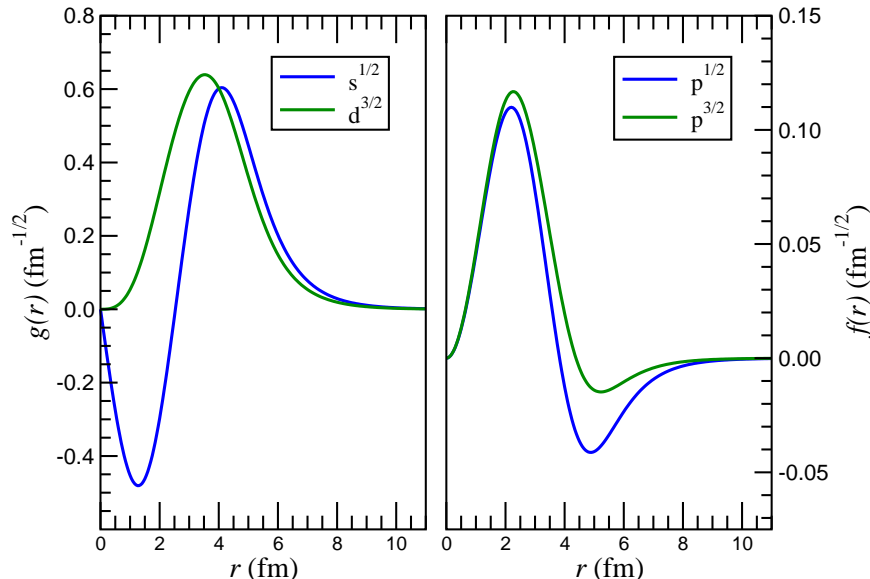


FIG. 2: (color online) Upper (left-hand panel) and lower (right-hand panel) components of the $2s^{1/2}$ and $1d^{3/2}$ proton orbitals in ^{48}Ca . The left-hand panel illustrates the different character of the upper components in the nuclear interior. In contrast, the right-hand panel accentuates the similarity among the corresponding lower components and provides a natural explanation for the appearance of pseudospin symmetry in nuclei.

In the present relativistic mean-field model the gradual return of the $1f^{7/2}$ -orbit to its parent $2p-1f$ shell is caused by the repulsive vector-isovector interaction. As the six protons are removed from the $2s^{1/2}-1d^{3/2}$ orbitals, the isovector interaction—which is driven by the difference between proton and neutron vector densities—becomes increasingly repulsive for neutrons, resulting in a ~ 2 MeV erosion of the $N = 28$ gap (see Table III). Such a significant reduction is likely to cause a redistribution of single-particle strength among the various neutron orbitals in the $2p-1f$ shell. This could become an important source of soft positive-parity (*e.g.*, quadrupole) excitations and/or deformation. Indeed, a preliminary random-phase-approximation (RPA) calculation of quadrupole strength based on the formalism outlined in Refs. [36, 37] reveals a low-lying 2^+ excitation at ~ 0.5 MeV in ^{42}Si .

The one aspect that remains to be addressed is the quenching of the spin-orbit splitting of the neutron p -orbitals as a function of proton $s^{1/2}$ removal. In Ref. [22] it was proposed that the depletion of $s^{1/2}$ strength could have a dramatic effect on the spin-orbit splitting of low angular momentum orbitals. In particular, it was demonstrated that the spin-orbit splitting of the $p^{3/2}-p^{1/2}$ neutron orbitals depends sensitively on the occupation of $s^{1/2}$ proton orbits. Two exotic nuclei were identified — ^{46}Ar and ^{206}Hg — in which the depletion of $s^{1/2}$ proton strength yields a dramatic quenching in the spin-orbit splitting of neutron p -orbitals near the Fermi surface. Since then, this prediction has been confirmed experimentally. Indeed, a significant weakening of the spin-orbit splitting among the $2p^{3/2}-2p^{1/2}$ neutron orbitals in ^{46}Ar has been reported recently by Gaudefroy, Sorlin, and collaborators [23]. We now demonstrate that the weakening of the spin-orbit splitting continues as one reaches ^{42}Si .

The weakening of the spin-orbit splitting among the neutron p -orbitals is clearly dis-

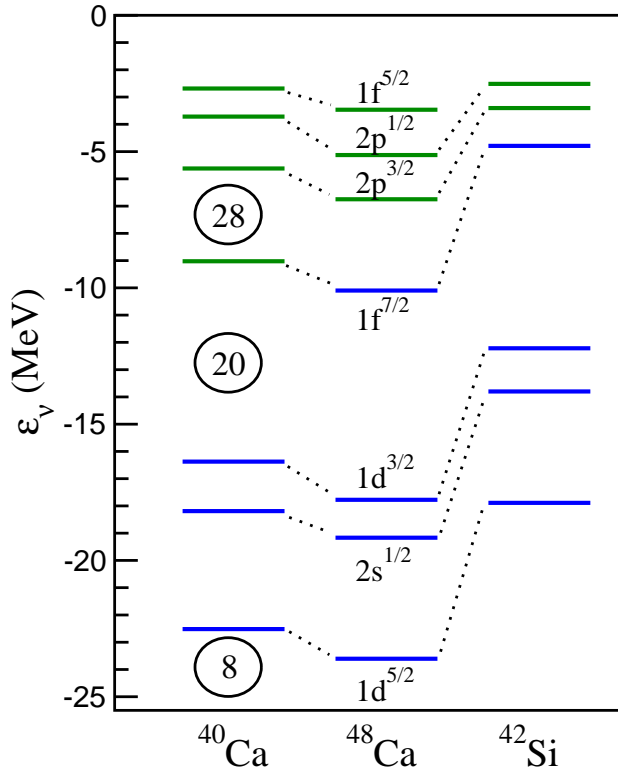


FIG. 3: (color online) Neutron single-particle spectrum in ^{40}Ca , ^{48}Ca , and ^{42}Si . Particularly relevant are: (i) the return of the $1f^{7/2}$ orbital to its parent shell in ^{42}Si and (ii) the $\sim 50\%$ reduction in the spin-orbit splitting of the p -orbitals in ^{42}Si relative to ^{48}Ca .

cernible in Fig. 3. The removal of the $2s^{1/2}$ protons is responsible for “carving” a hole in the nuclear interior that dramatically reshapes the spin-orbit potential, leaving a strong imprint on neutron orbitals of low angular momentum [22]. The development of a proton hole in the nuclear interior as $2s^{1/2}$ protons are progressively removed is nicely illustrated in Fig. 4. Note that a uniform filling fraction of $2/3$ and $1/3$ has been assumed for ^{46}Ar and ^{44}S , respectively. This choice is motivated by the quasi-degeneracy of the $1d^{3/2}$ - $2s^{1/2}$ orbitals.

In Fig. 5 we display the sensitivity of the spin-orbit splitting among neutron p -orbitals to the filling fraction of the proton $2s^{1/2}$ orbit. The removal of $2s^{1/2}$ strength yields a sharp increase in the magnitude of the spin-orbit interaction in the nuclear interior that cancels part of the surface contribution. One can observe that in the case that only $1d^{3/2}$ protons are removed [$n_\pi(2s^{1/2}) \equiv 1$] the model actually predicts a slight increase in the spin-orbit splitting. Yet the more plausible assumption of a uniform proton removal from the quasi-degenerate orbits leads to a spin-orbit quenching of about 20% and 30% for ^{46}Ar and ^{44}S , respectively. These values are indicated as stars in the figure. In the case of ^{42}Si , where the $2s^{1/2}$ removal is complete, the spin-orbit quenching reaches almost 50%. Note that while the quenching of the spin-orbit splitting is a robust prediction of the relativistic mean-field model—as the interior contribution to the spin-orbit potential always works against the dominant surface contribution—the precise magnitude of the quenching is model dependent.

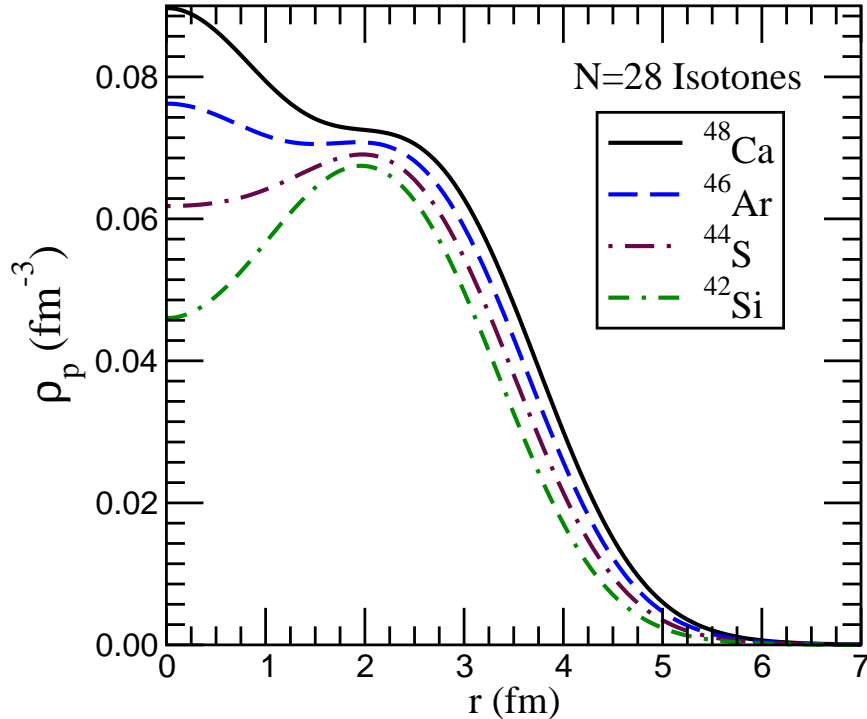


FIG. 4: (color online) Point proton densities for the four $N=28$ isotones considered in the text. The development of a proton “hole” in the nuclear interior is responsible for the weakening of the spin-orbit splitting among the neutron p -orbitals.

Nucleus	$\epsilon(1f^{7/2})$ (MeV)	$\epsilon(2p^{3/2})$ (MeV)	$\epsilon(2p^{1/2})$ (MeV)
^{48}Ca	-10.10 (4.97)	-6.75 (1.62)	-5.13 (0.00)
^{46}Ar	-8.35 (4.13)	-5.57 (1.35)	-4.22 (0.00)
^{44}S	-6.58 (3.24)	-4.45 (1.11)	-3.34 (0.00)
^{42}Si	-4.79 (2.27)	-3.41 (0.89)	-2.52 (0.00)

TABLE III: Evolution of the neutron $p-f$ shell with proton removal from the $1d^{3/2}$ and $2s^{1/2}$ orbitals. Quantities in parenthesis are single-neutron energies relative to the $\epsilon(2p^{1/2})$.

For example, the original NL3 parameter set predicts a $2p^{1/2}$ - $2p^{3/2}$ splitting in ^{46}Ar at zero $2s^{1/2}$ filling of only 0.17 MeV [22], rather than the 0.67 MeV value obtained here with the slightly modified parameter set.

IV. CONCLUSIONS

A study of the $N=28$ isotonic chain was conducted within the framework of the relativistic mean-field approximation. For our calculations, we relied on a slightly modified NL3 parameter set [28]. While accurately calibrated and highly successful in describing a variety of ground state observables [29], the original NL3 set underestimates the $1d^{3/2}$ - $2s^{1/2}$

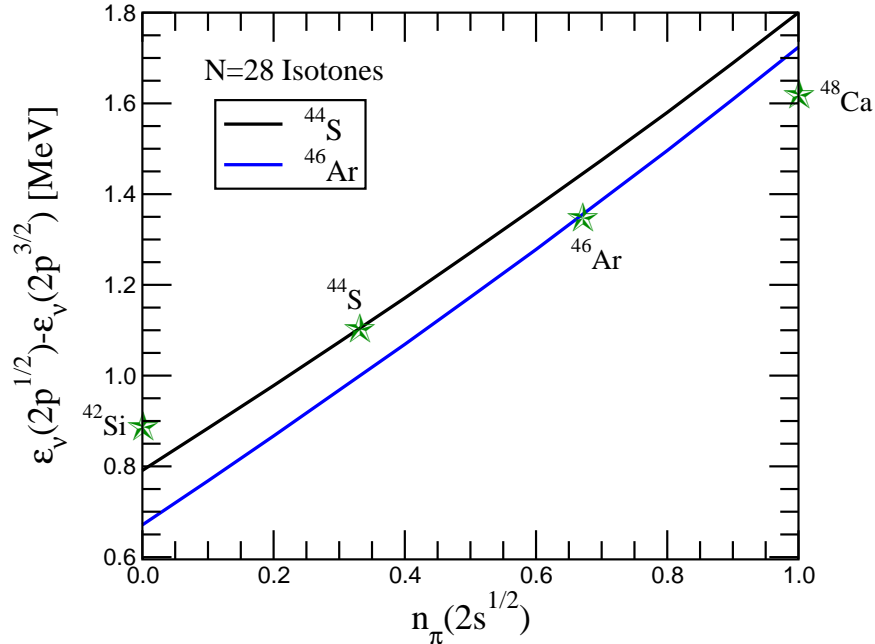


FIG. 5: Spin-orbit splitting of the neutron p -orbitals as a function of the proton $2s^{1/2}$ occupancy for the four $N=28$ isotones considered in the text. Values indicated with a “star” for ^{44}S and ^{46}Ar have been obtained by assuming a uniform occupancy of the quasi-degenerate $2s^{1/2}$ - $1d^{3/2}$ proton orbitals.

proton gap (~ 800 keV *vs* ~ 2 MeV) in ^{40}Ca . Thus, a fine tuning of the NL3 parameter set was performed to properly account for the gap. The adjustments were done in such a way that the binding energy and charge radius of ^{40}Ca remain close to their experimental values. This adjustment, alone and with nothing else, yields a nearly degenerate $1d^{3/2}$ - $2s^{1/2}$ proton pair and a robust $Z=14$ gap in ^{48}Ca , in agreement with experiment.

The aim of the present study was threefold. First, to determine if the appearance of a new magic number at $Z=14$ in ^{48}Ca persists as one reaches ^{42}Si [3]. Second, to explore the persistence—or lack thereof—of the $N=28$ shell closure in ^{42}Si [15, 17, 18, 20, 21, 34]. Finally, to monitor the weakening of the spin-orbit splitting of the $2p^{3/2}$ - $2p^{1/2}$ neutron orbits as a function of the occupancy of the $2s^{1/2}$ proton orbital [22, 23].

Regarding the first topic, we found that the addition of 8 neutrons to the $1f^{7/2}$ orbit reduces the $1d^{3/2}$ - $2s^{1/2}$ proton gap from ~ 2 MeV in ^{40}Ca to a mere 110 keV in ^{48}Ca . This, in turn, yields a robust ~ 6 MeV energy gap at proton number $Z=14$. As the removal of all 6 protons from the degenerate $1d^{3/2}$ - $2s^{1/2}$ orbitals weakens the $Z=14$ gap only slightly (by ~ 1 MeV), our results support the emergence of a well developed proton subshell closure at $Z=14$ [3].

Yet the present relativistic mean-field model predicts that as protons are progressively removed from the $1d^{3/2}$ - $2s^{1/2}$ orbitals, the $1f^{7/2}$ neutron orbit returns to its parent fp -shell—leading to the disappearance of the magic number $N=28$. In the present model the $N=28$ gap is systematically reduced from 3.4 MeV in ^{48}Ca , to 2.8 MeV in ^{46}Ar , to 2.1 MeV in ^{44}S , and ultimately to 1.4 MeV in ^{42}Si . The significant reduction in the gap is caused by

the Lorentz structure of the isovector interaction, assumed here to be of vector character. For neutron-rich nuclei, a vector-isovector structure generates repulsion for the majority species (neutrons) and attraction for the minority species (protons). Thus, in the present model the proton removal is ultimately responsible for the return of the $1f^{7/2}$ neutron orbit to its parent shell. It is conceivable that the disappearance of the $N = 28$ magic number could promote both deformation and/or soft quadrupole excitations. Indeed, some of our preliminary RPA calculations suggest a low-energy quadrupole excitation at around 500 keV. Yet the ultimate shape of ^{42}Si —either spherical [3, 15, 34] or deformed [18, 20, 21]—its single-particle structure, and the character of its low-energy excitations, will continue to be the source of considerable debate for years to come.

Finally, the weakening of the spin-orbit splitting among low- j neutron orbits—an effect first predicted for p -orbitals in ^{46}Ar and ^{206}Hg [22], and recently confirmed experimentally in ^{46}Ar [23]—is strongly correlated to the occupancy of the proton $2s^{1/2}$ orbital. Indeed, the removal of $s^{1/2}$ strength induces significant structure in the nuclear interior that is responsible for canceling part of the dominant surface contribution to the spin-orbit potential. This cancellation yields a significant quenching of $\sim 50\%$ in the spin-orbit splitting of the $2p$ neutron orbitals in ^{42}Si relative to the corresponding splitting in ^{48}Ca .

Acknowledgments

The author gratefully acknowledges Professors P. Cottle, O. Sorlin, A. Volya, and I. Wiedenhover for valuable discussions and illuminating insights. This work was supported in part by DOE grant DE-FG05-92ER40750.

-
- [1] W. Nazarewicz and R. F. Casten, Nucl. Phys. **A682**, 295c (2001).
 - [2] J. Dobaczewski and W. Nazarewicz, Prog. Theor. Phys. Suppl. **146**, 70 (2003), nucl-th/0203038.
 - [3] J. Fridmann et al., Nature **435**, 922 (2005).
 - [4] P. T. Hosmer et al., Phys. Rev. Lett. **94**, 112501 (2005), nucl-ex/0504005.
 - [5] G. J. Mathews and J. J. Cowan, Nature **345**, 491 (1990).
 - [6] K.-L. Kratz, B. Pfeiffer, F.-K. Thielemann, and W. B. Walters (1999), astro-ph/9907071.
 - [7] F. K. Thielemann et al., Prog. Part. Nucl. Phys. **46**, 5 (2001), astro-ph/0101476.
 - [8] B. A. Brown, Phys. Rev. Lett. **85**, 5296 (2000).
 - [9] R. J. Furnstahl, Nucl. Phys. **A706**, 85 (2002), nucl-th/0112085.
 - [10] C. J. Horowitz and J. Piekarewicz, Phys. Rev. Lett. **86**, 5647 (2001), astro-ph/0010227.
 - [11] C. J. Horowitz and J. Piekarewicz, Phys. Rev. **C64**, 062802 (2001), nucl-th/0108036.
 - [12] J. Carriere, C. J. Horowitz, and J. Piekarewicz, Astrophys. J. **593**, 463 (2003), nucl-th/0211015.
 - [13] C. J. Horowitz and J. Piekarewicz, Phys. Rev. **C66**, 055803 (2002), nucl-th/0207067.
 - [14] S. Grevy et al., Phys. Lett. **B 594**, 252 (2004).
 - [15] J. Retamosa, E. Caurier, F. Nowacki, and A. Poves, Phys. Rev. **C55**, 1266 (1997), nucl-th/9608003.
 - [16] E. Caurier, F. Nowacki, and A. Poves, Nucl. Phys. **A742**, 14 (2004), nucl-th/0403080.
 - [17] T. R. Werner et al., Phys. Lett. **B333**, 303 (1994), nucl-th/9406013.
 - [18] T. R. Werner et al., Nucl. Phys. **A597**, 327 (1996).
 - [19] J. Terasaki, H. Flocard, P. H. Heenen, and P. Bonche, Nucl. Phys. **A621**, 706 (1997), nucl-th/9612058.
 - [20] G. A. Lalazissis, D. Vretenar, P. Ring, M. Stoitsov, and L. Robledo, Phys. Rev. **C60**, 014310 (1999), nucl-th/9807029.
 - [21] S. Péru, M. Girod, and J. F. Berger, Eur. Phys. J. **A9**, 35 (2000).
 - [22] B. G. Todd-Rutel, J. Piekarewicz, and P. D. Cottle, Phys. Rev. **C69**, 021301 (2004).
 - [23] L. Gaudefroy et al., Phys. Rev. Lett. **xxx**, xxx (2006).
 - [24] T. Otsuka et al., Phys. Rev. Lett. **87**, 082502 (2001), nucl-th/0107054.
 - [25] T. Otsuka et al., Phys. Rev. Lett. **95**, 232502 (2005).
 - [26] S. Milena, O. T. Otsuka, A. Yoshinori, R. Peter, and H. Shunsuke, Prog. Theor. Phys. **113**, 1009 (2005).
 - [27] R. J. Furnstahl and B. D. Serot, Comments Nucl. Part. Phys. **2**, A23 (2000), nucl-th/0005072.
 - [28] G. A. Lalazissis, J. Konig, and P. Ring, Phys. Rev. **C55**, 540 (1997), nucl-th/9607039.
 - [29] G. A. Lalazissis, S. Raman, and P. Ring, At. Data Nucl. Data Tables **71**, 1 (1999).
 - [30] B. D. Serot and J. D. Walecka, Adv. Nucl. Phys. **16**, 1 (1986).
 - [31] B. D. Serot and J. D. Walecka, Int. J. Mod. Phys. **E6**, 515 (1997), nucl-th/9701058.
 - [32] B. G. Todd and J. Piekarewicz, Phys. Rev. **C67**, 044317 (2003), nucl-th/0301092.
 - [33] G. J. Kramer, Ph.D. thesis, University of Amsterdam (1990).
 - [34] P. D. Cottle and K. W. Kemper, Phys. Rev. **C58**, 3762 (1998).
 - [35] J. Piekarewicz, Phys. Rev. **C48**, 2174 (1993), nucl-th/9306011.
 - [36] J. Piekarewicz, Phys. Rev. **C62**, 051304 (2000), nucl-th/0003029.
 - [37] J. Piekarewicz, Phys. Rev. **C64**, 024307 (2001), nucl-th/0103016.